

**ORIGINAL ARTICLE****Time series of optical spectra of Nova V659 Sct**Dennis Jack\*<sup>1</sup> | Klaus-Peter Schröder<sup>1,2</sup> | Philippe Eenens<sup>1</sup> | Uwe Wolter<sup>3</sup> | José Nicolás González-Pérez<sup>3</sup> | Jürgen H. M. M. Schmitt<sup>3</sup> | Peter H. Hauschildt<sup>3</sup><sup>1</sup>Departamento de Astronomía, Universidad de Guanajuato, Guanajuato, Mexico<sup>2</sup>Sterrewacht Leiden, Universiteit Leiden, Leiden, Netherlands<sup>3</sup>Hamburger Sternwarte, Universität Hamburg, Hamburg, Germany**Correspondence**

\*Dennis Jack, Email: dennis.jack@ugto.mx

**Present Address**

Departamento de Astronomía, Universidad de Guanajuato, A.P. 144, 36000 Guanajuato, GTO, Mexico

With our robotic 1.2 m TIGRE telescope, we were able to obtain eight optical spectra with intermediate resolution ( $R \approx 20,000$ ) of the Nova V659 Sct during different phases of its outburst. We present a list of the lines found in the Nova spectra. The most common features are H I, O I, Na I, Fe II and Ca II. Studying the spectral evolution of the strong features we found that the absorption features move to higher expansion velocities before disappearing and the emission features show (different) asymmetries. Thanks to the intermediate spectral resolution we identified and analysed the interstellar medium absorption features present in the spectra. We detected atomic absorption features of Na I and Ca II. The sodium D lines show more complex substructures with three main absorption features at around a velocity of  $-10$ ,  $30$  and  $85 \text{ km s}^{-1}$ . We identified several DIBs in the Nova V659 Sct spectra and determined their velocities and equivalent widths.

**KEYWORDS:**

stars: novae, cataclysmic variables – stars: individual: Nova V659 Sct – techniques: spectroscopic – line: identification

**1 | INTRODUCTION**

The occasional appearance of "new stars" (Stella Nova) in the sky are bright outbursts known today as classical novae which are the result of the accretion process in a close binary system consisting of a white dwarf (WD) and its main sequence or evolved companion star. The WD accumulates hydrogen from the companion star on its surface which eventually ignites and explodes in a thermonuclear runaway. During this outburst the brightness of the WD increases by several magnitudes and one can observe these events as classical novae with their typical light curves and spectral evolution (see Bode (2010); Bode & Evans (2008); Gallagher & Starrfield (1978); Payne-Gaposchkin (1964) or Starrfield, Iliadis, & Hix (2016) for reviews).

The galactic Nova V659 Sct (Nova Scuti 2019, AT 2019tpb, ASASSN-19aad, TCP J18395972-1025415) was discovered on October 29.058 UT (Stanek & Kochanek, 2019) by the

ASAS-SN survey (Kochanek et al., 2017; Shappee et al., 2014) in the constellation Scutum. An independent discovery was reported by Nishiyama, Kabashima, & Nishimura (2019) a few hours later. Nova V659 Sct was quickly identified as a classical nova in its early stages of the outburst (Williams, Darnley, Healy, Murphy-Glaylor, & Ransome, 2019). This nova had a  $V$  band brightness of 8.4 mag during maximum optical light, a bright event which could be observed also by small and medium-sized telescopes. However, its position close to the Sun in the sky made it somewhat difficult to observe. Optical spectra were reported by Pavana, Anupama, & Kumar (2019) showing the typical lines for a classical nova with the common P-Cygni profiles. Observations with the SWIFT telescope were performed (Sokolovsky et al., 2019). The nova outburst was detected by instruments, both, in X-rays and the UV wavelength range. Sokolovsky et al. (2019) determined that the nova was affected by galactic reddening of about  $E(B - V) = 0.9$ .

Our robotic 1.2 m TIGRE telescope is an ideal instrument for the observation of time series of bright nova and

<sup>0</sup>Abbreviations:

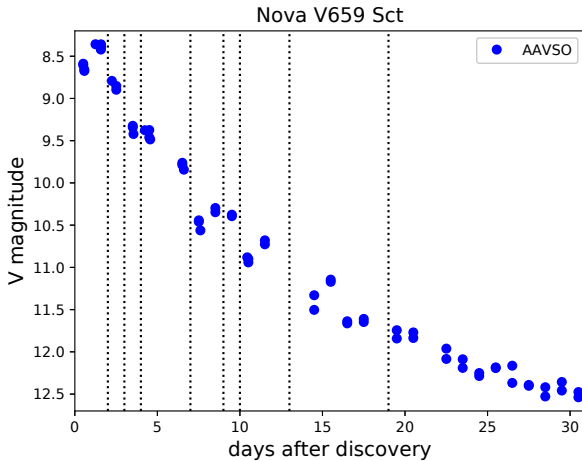


**FIGURE 1** The  $V$  band light curve of Nova V659 Sct. The data points were taken from AAVSO observations. Vertical lines mark TIGRE observations.

even supernova events, like SN 2014J (Jack et al., 2015). Nova V659 Sct is the third nova that we could observe with our intermediate resolution optical spectrograph. So far, we have obtained time series of the two classical Novae V339 Del (De Gennaro Aquino et al., 2015) and V5668 Sgr (Jack et al., 2017).

The paper is structured as follows. We will present in Section 2 details about the observations of the optical spectra of Nova V659 Sct that we obtained with the TIGRE telescope. An analysis of the observed spectra including a line identification, also for interstellar absorption features, is presented in Section 3. We will close the presentation of our work with a summary in Section 4.

## 2 | OBSERVATIONS OF NOVA V659 SCT

### 2.1 | $V$ band light curve

In Figure 1, we present the  $V$  band light curve of Nova V659 Sct using the prevalidated observations published by the AAVSO on its website<sup>1</sup>. The position of the Nova in the constellation of Scutum was close to the Sun on the sky, and after about 30 days the Nova was not observable any more. Nova V659 Sct was discovered before its the maximum optical light, which was reached around October 31, 2019. After the maximum the brightness dropped about 4 magnitudes over the following 30 days. The vertical lines in Figure 1 mark the observation times where we obtained optical spectra with the TIGRE telescope. We were able to take the first spectrum about

two days after the discovery during the maximum phase of the  $V$  band light curve. Our last spectrum was obtained about 19 days after discovery because after that the Nova was too close to the Sun on the sky which did not allow us to have sufficient exposure time.

We applied the maximum magnitude versus rate of decline (MMRD) relationship of della Valle & Livio (1995) to estimate the distance to Nova V659 Sct. Using  $E(B - V) = 0.9$  (Sokolovsky et al., 2019) and assuming  $R_V = 3.1$  we obtained an extinction of  $A_V = 2.8$  mag. From the  $V$  band light curve we determined its maximum brightness to have a value of  $m_V = 8.35$  mag. It is not possible to determine the time for the decline of 2 magnitudes very precisely because of few measurements and large scatter in the light curve. We assumed a value of  $t_2 = 7.5$  days. Applying the MMRD relation we obtained an absolute visual magnitude for Nova V659 Sct of  $M_V = -8.8$  mag and, thus, a distance of 7.5 kpc to it. In order to verify this result we looked at the 3D Dust Mapping<sup>2</sup> (Green, Schlafly, Zucker, Speagle, & Finkbeiner, 2019). In the direction of Nova V659 Sct, the distance of 7.5 kpc corresponds to an extinction of  $E(g - r) = 0.96$ , which roughly coincides with the before mentioned  $E(B - V) = 0.9$ .

### 2.2 | TIGRE observations

The observations were carried out with the TIGRE (Telescopio Internacional de Guanajuato Robotico Espectroscopico) telescope at the observatory of La Luz located close to the town of Guanajuato in Central Mexico. TIGRE is a robotic telescope with a mirror of an aperture of 1.2 m. The HEROS (Heidelberg Extended Optical Range Spectrograph) echelle spectrograph has an intermediate resolution of about  $R \approx 20,000$  and obtains optical spectra in the wavelength range from about 3,800 to 8,800 Å, having a small gap of about 120 Å between the two arms around 5,800 Å. Thus, the observed spectra are divided into two channels (blue and red). All observations and the data reduction are performed automatically, which includes the barycentric correction. For more technical details about the TIGRE telescope, consult Schmitt et al. (2014).

Due to weather conditions we could obtain the first spectrum during the night of October 31, 2019. In total, we obtained eight optical spectra of Nova V659 Sct during different phases of the spectral evolution. Fortunately, we were able to take three spectra during consecutive nights. Our last spectrum was taken on November 17, about 19 days after the discovery. The details of our observation campaign can be found in Table A1.

A set of six of the observed spectra of Nova V659 Sct is shown for the blue channel in Figure 2. The spectrum from November 8 shows very small differences to the one from

<sup>1</sup><https://www.aavso.org/>

<sup>2</sup><http://argonaut.skymaps.info/>

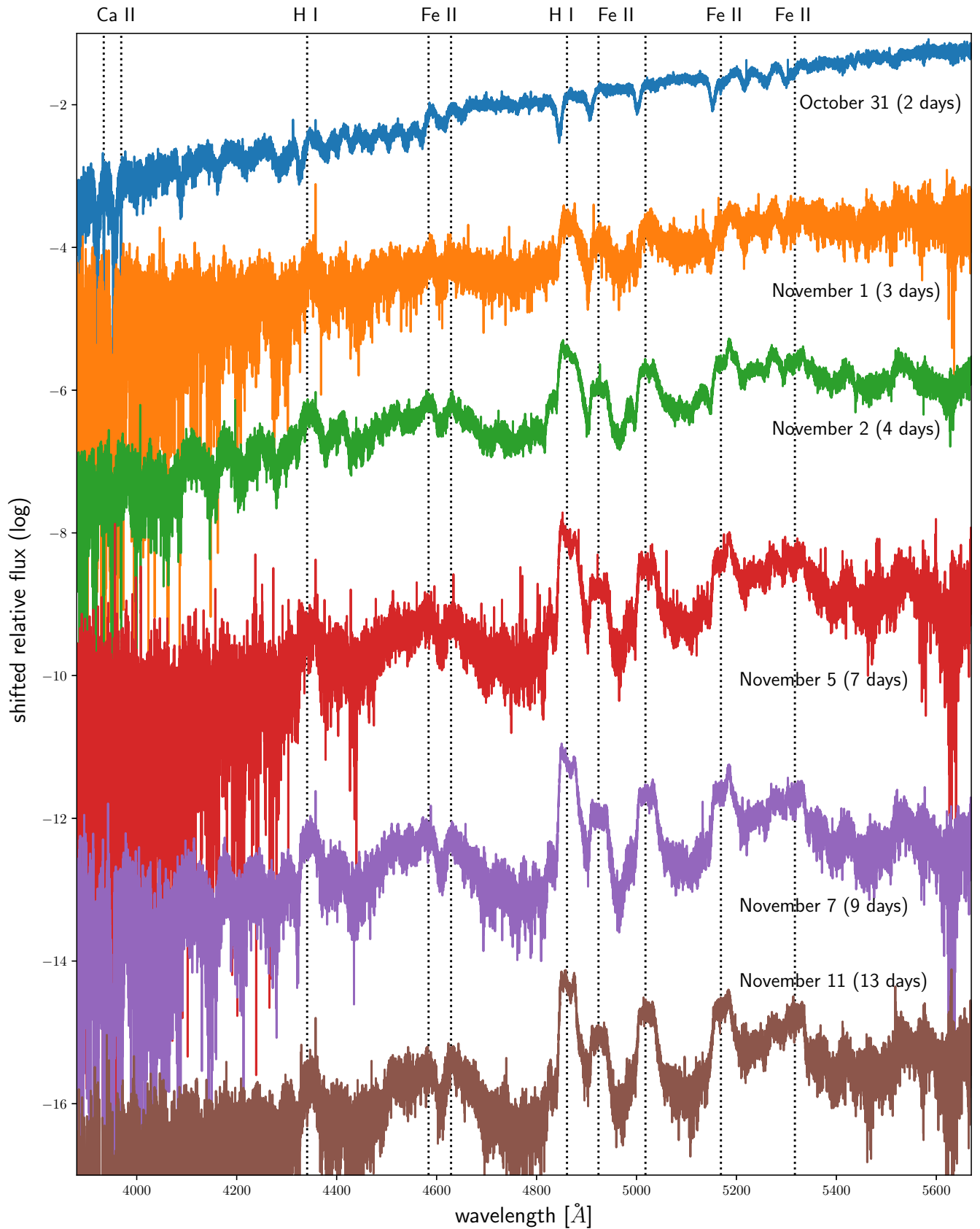


**FIGURE 2** Six spectra of Nova V659 Set observed in the blue channel of the HEROS spectrograph. Dates are of 2019 and the corresponding days after discovery are given in brackets. The part below 4400  $\text{\AA}$  suffers from very low S/N.

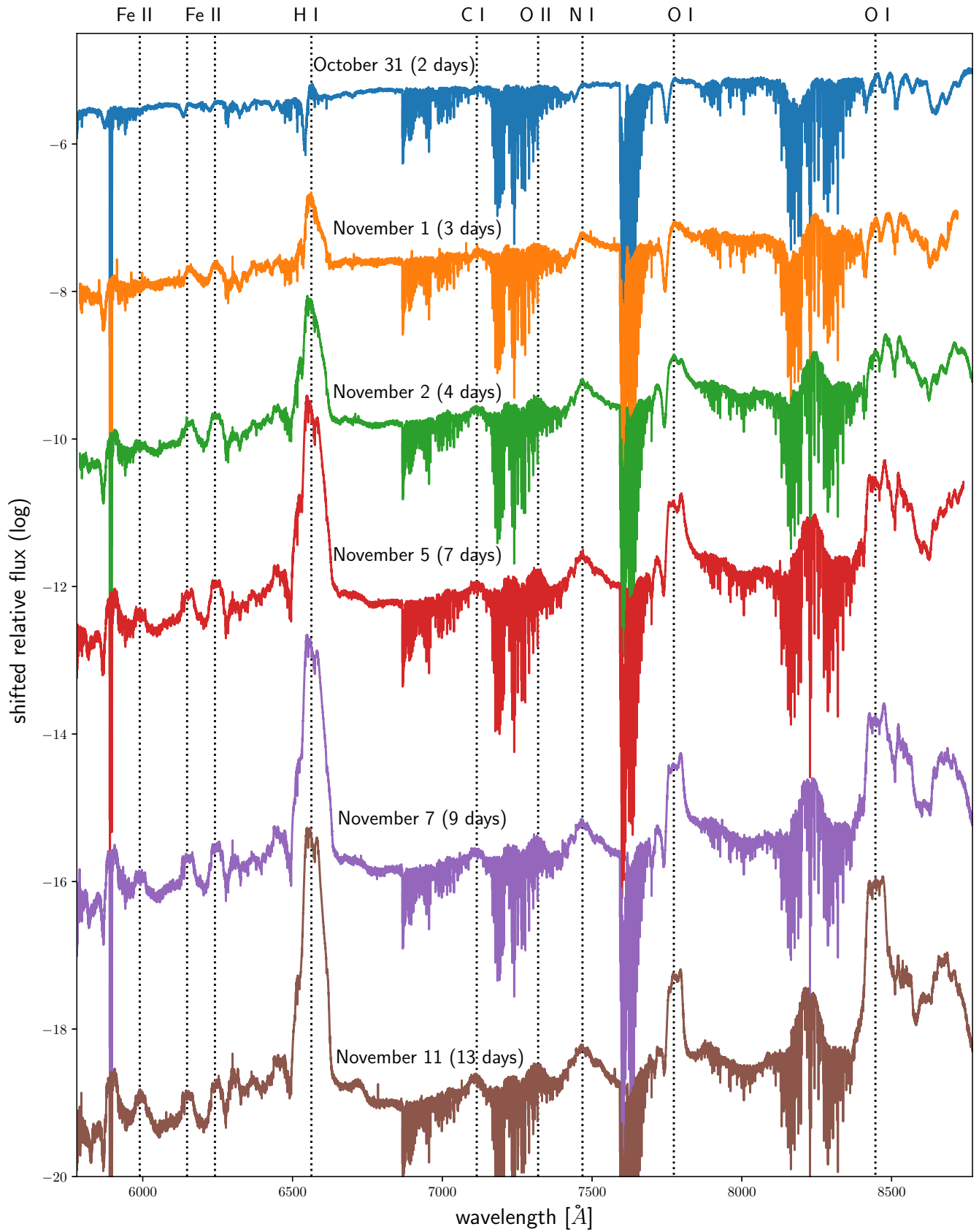


**FIGURE 3** Six spectra of Nova V659 Sct observed in the red channel of the HEROS spectrograph. Dates are of 2019 and the corresponding days after discovery are given in brackets. Broad bands of telluric lines are present in this wavelength range.

November 7, and the spectrum from November 17 had a very low signal-to-noise ratio and no features are visible in the blue channel. For those reasons we here present only six spectra. The presented spectra highlight the different phases of the nova outburst. The first spectrum is still in the absorption phase and was taken during the maximum of the  $V$  band light curve. The next spectrum, taken one night later, shows P-Cygni profile lines. The later spectra show the evolution towards the emission line phase. We marked the most important features in the Nova V659 Sct spectra with vertical lines at their rest wavelengths. One can clearly see the blueshifted absorption features of each line, while the emission features are centered around the rest wavelengths. In the blue channel, we clearly identify features of Ca II, Fe II and H I. Since the Nova was close to the Sun on the sky, we were not able to make long exposures right after sunset also with the nova being hardly above the horizon. As a result, several wavelength regions of the blue part of some of the spectra are affected by noise and the lines are not always visible.

Six observed TIGRE spectra in the red channel are presented in Figure 3. The spectra have a higher signal-to-noise ratio (S/N) than in the blue channel. However, in this wavelength range some regions of the spectra are contaminated by the broad telluric absorption bands. The red spectra contain the common features of Fe II and H I as well as some lines of O I, O II and N I. Here, the first spectrum shows already P-Cygni profiles. This may have to do with the spectral energy distribution since bluewards of the maximum flux the features are often in absorption, while redwards it is P-Cygni profiles or emission. The strongest features are the  $H\alpha$  line and the two lines of O I at 7773.0 Å and 8446.3 Å, which show asymmetric emission during the later phase of the spectral evolution. The narrow and deep absorption feature around 5900 Å is interstellar absorption of the Na I doublet lines.

### 3 | SPECTRAL ANALYSIS

Having eight TIGRE spectra of Nova V659 Sct with an intermediate resolution allows us to analyse them in detail and identify and study the features present in the Nova. In addition, we are able to study the absorption features of the interstellar medium in form of atomic lines and DIBs. We present the results in this following section.

#### 3.1 | Line identification

We thoroughly inspected all the above presented six optical spectra taken of Nova V659 Sct and identified all features in these spectra using the database of lines found in Nova V339 Del and published in De Gennaro Aquino et al. (2015).

**TABLE 1** List of lines in the blue channel that have been identified in the six observed spectra of Nova V659 Sct.

| Line [Å] | Ion     | Oct 31 | Nov 1 | Nov 2 | Nov 5 | Nov 7 | Nov 11 |
|----------|---------|--------|-------|-------|-------|-------|--------|
| 3835.4   | H I     | ✓      |       |       |       |       |        |
| 3889.1   | H I     | ✓      |       |       |       |       |        |
| 3933.7   | Ca II   | ✓      | ✓     | ✓     |       | ✓     |        |
| 3968.5   | Ca II   | ✓      | ✓     | ✓     |       | ✓     |        |
| 3970.1   | H I     | ✓      | ✓     | ✓     |       | ✓     |        |
| 4101.7   | H I     | ✓      |       |       |       | ✓     | ✓      |
| 4130.9   | Si II   | ✓      |       |       |       |       |        |
| 4173.5   | Fe II   | ✓      |       | ✓     |       | ✓     | ✓      |
| 4178.9   | Fe II   | ✓      |       | ✓     |       | ✓     | ✓      |
| 4233.2   | Fe II   | ✓      |       |       |       | ✓     | ✓      |
| 4296.5   | Fe II   | ✓      |       |       |       | ✓     | ✓      |
| 4340.5   | H I     | ✓      | ✓     | ✓     | ✓     | ✓     | ✓      |
| 4385.4   | Fe II   | ✓      | ✓     |       |       |       |        |
| 4416.3   | Fe II   | ✓      | ✓     | ✓     |       |       |        |
| 4416.8   | [Fe II] | ✓      | ✓     | ✓     |       |       |        |
| 4443.8   | Ti II   | ✓      |       |       |       |       |        |
| 4481.2   | Mg II   | ✓      |       |       |       |       |        |
| 4522.6   | Fe II   | ✓      |       |       |       |       |        |
| 4555.8   | Fe II   | ✓      |       |       |       |       |        |
| 4583.8   | Fe II   | ✓      | ✓     | ✓     | ✓     | ✓     | ✓      |
| 4629.3   | Fe II   | ✓      | ✓     | ✓     | ✓     | ✓     | ✓      |
| 4670.4   | Sc II   | ✓      |       |       |       |       |        |
| 4772.1   | [Fe II] | ✓      |       |       |       |       |        |
| 4805.1   | Ti II   | ✓      |       |       |       |       |        |
| 4861.3   | H I     | ✓      | ✓     | ✓     | ✓     | ✓     | ✓      |
| 4923.9   | Fe II   | ✓      | ✓     | ✓     | ✓     | ✓     | ✓      |
| 5018.4   | Fe II   | ✓      | ✓     | ✓     | ✓     | ✓     | ✓      |
| 5129.2   | Ti II   | ✓      |       |       |       |       |        |
| 5169.0   | Fe II   | ✓      | ✓     | ✓     | ✓     |       |        |
| 5197.6   | Fe II   | ✓      | ✓     |       |       |       |        |
| 5234.6   | Fe II   | ✓      | ✓     | ✓     |       |       |        |
| 5276.0   | Fe II   | ✓      | ✓     | ✓     | ✓     | ✓     | ✓      |
| 5316.6   | Fe II   | ✓      | ✓     | ✓     | ✓     | ✓     | ✓      |
| 5362.8   | Fe II   | ✓      |       |       |       |       |        |
| 5425.0   | Fe II   |        |       | ✓     | ✓     |       |        |
| 5532.1   | Fe II   | ✓      | ✓     | ✓     | ✓     | ✓     | ✓      |

We present the list of lines that we identified in the blue channel of the HEROS spectrograph of Nova V659 Sct in Table 1. Since the spectrum from November 8 is almost the same as the one from November 7 the identified lines in the spectrum from November 7 are also visible in the spectrum from November 8. The spectrum from November 17 is only noise in the blue channel, and no lines are visible. Below 4400 Å some of the spectra have a very low signal-to-noise ratio, because of the low flux and the relatively short exposure

**TABLE 2** List of lines in the red channel that have been identified in the six observed spectra of Nova V659 Sct.

| Line [ $\text{\AA}$ ] | Ion    | Oct 31 | Nov 1 | Nov 2 | Nov 5 | Nov 7 | Nov 11 |
|-----------------------|--------|--------|-------|-------|-------|-------|--------|
| 5875.6                | He I   |        |       |       | ✓     | ✓     |        |
| 5889.9                | Na I   | ✓      | ✓     | ✓     | ✓     | ✓     | ✓      |
| 5895.9                | Na I   | ✓      | ✓     | ✓     | ✓     | ✓     | ✓      |
| 5991.4                | Fe II  |        |       |       | ✓     | ✓     | ✓      |
| 6148.0                | Fe II  | ✓      | ✓     | ✓     | ✓     | ✓     | ✓      |
| 6240.6                | Fe II  | ✓      | ✓     | ✓     | ✓     | ✓     | ✓      |
| 6247.6                | Fe II  | ✓      | ✓     | ✓     | ✓     | ✓     | ✓      |
| 6300.3                | [O I]  | ✓      | ✓     | ✓     | ✓     | ✓     | ✓      |
| 6347.1                | Si II  | ✓      |       |       |       |       |        |
| 6371.4                | Si II  | ✓      | ✓     | ✓     | ✓     | ✓     | ✓      |
| 6456.4                | Fe II  | ✓      | ✓     |       |       |       |        |
| 6483.8                | Ni II  | ✓      | ✓     |       |       |       |        |
| 6562.7                | H I    | ✓      | ✓     | ✓     | ✓     | ✓     | ✓      |
| 6678.2                | He I   |        | ✓     | ✓     | ✓     | ✓     | ✓      |
| 6722.6                | N I    | ✓      | ✓     |       |       | ✓     | ✓      |
| 7115.0                | C I    | ✓      | ✓     | ✓     | ✓     | ✓     | ✓      |
| 7320.0                | [O II] |        |       | ✓     | ✓     | ✓     | ✓      |
| 7442.3                | N I    | ✓      | ✓     |       |       |       |        |
| 7468.2                | N I    | ✓      | ✓     | ✓     | ✓     | ✓     | ✓      |
| 7773.0                | O I    | ✓      | ✓     | ✓     | ✓     | ✓     | ✓      |
| 8220.0                | Fe II  | ✓      | ✓     | ✓     | ✓     | ✓     | ✓      |
| 8446.3                | O I    | ✓      | ✓     | ✓     | ✓     | ✓     | ✓      |
| 8498.0                | Ca II  | ✓      | ✓     | ✓     |       |       |        |
| 8542.1                | Ca II  | ✓      | ✓     | ✓     |       |       |        |
| 8598.4                | H I    | ✓      |       |       |       |       |        |
| 8662.1                | Ca II  | ✓      | ✓     | ✓     |       |       |        |
| 8665.0                | H I    | ✓      | ✓     | ✓     |       |       |        |
| 8750.5                | H I    | ✓      |       |       |       |       |        |

times due to the short observable time of the Nova on the sky right after sunset. Therefore, some features probably do not disappear but are just not clearly visible above the strong noise. Especially, the second spectrum from November 1, had a very low S/N due to bad weather conditions. The spectra of Nova V659 Sct contain many Fe II lines. The common hydrogen lines like  $H\beta$  are clearly visible. In addition, we could identify lines of Ca II, Si II, Ti II and Mg II. We also identified two forbidden lines. In summary, some lines disappear quickly during the spectral evolution, while the strong lines are visible in every spectrum up to the emission line phase.

The features we could identify in the red channel of the observed spectra of Nova V659 Sct are presented in Table 2. Apart from the prominent  $H\alpha$  line and the strong O I feature at 7773.0  $\text{\AA}$ , we found in the red channel spectra many lines of Fe II. In addition, we could identify lines of O II, Na I, Si II, Ni II, Ca II, C I and N I. We also identified two forbidden lines.

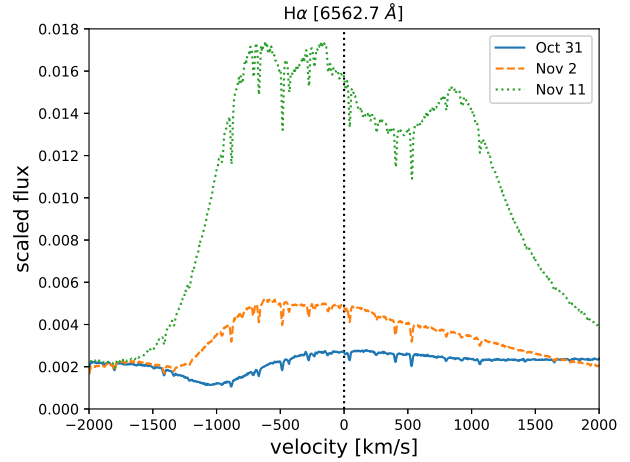


**FIGURE 4** Spectral evolution of the  $H\alpha$  feature. The narrow lines come from telluric absorption.

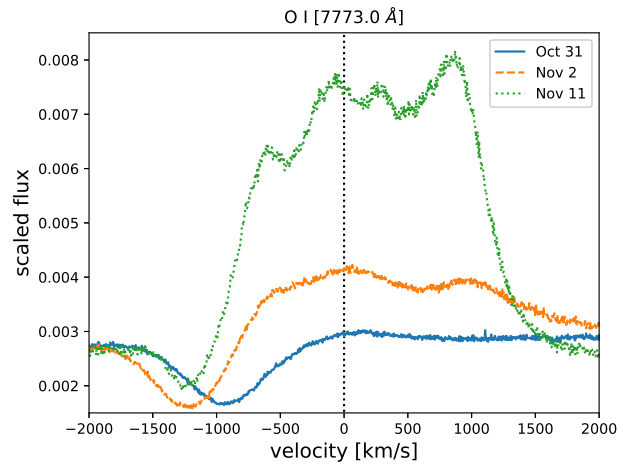


**FIGURE 5** Spectral evolution of O I feature at 7773.0  $\text{\AA}$ .

In the later spectra the features of the Ca II triplet and the H I line around 8500  $\text{\AA}$  are strongly blended and one cannot distinguish and clearly identify the contribution from each one of these lines to the broad emission feature observed at that wavelength. There could also be some features hidden in the strong absorption bands of telluric lines present in the red channel of the spectra of Nova V659 Sct. In the low S/N spectrum from November 17 only three features of the  $H\alpha$  line and two O I lines at 7773.0 and 8446.3  $\text{\AA}$  are visible.

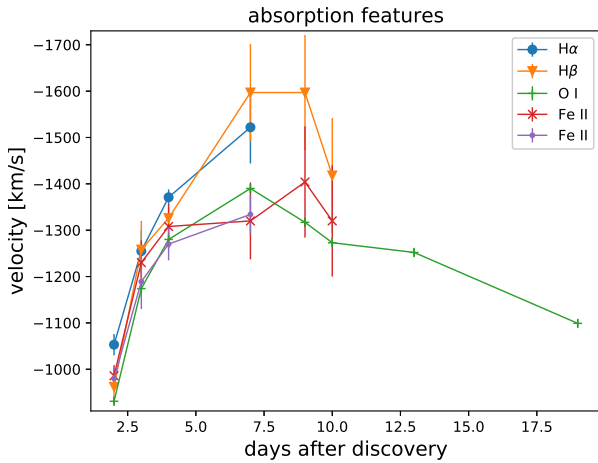


**FIGURE 6** Evolution of the expansion velocities of the absorption features of five spectral lines that correspond to three different species.

### 3.2 | Spectral evolution of prominent features

To present some examples for the spectral evolution of the features in the spectra of Nova V659 Sct, in Figure 4, we show three spectra of the prominent  $H\alpha$  line. The first spectrum from October 31 shows a clear absorption feature around  $-1000 \text{ km s}^{-1}$ . Two days later, the absorption feature has moved bluewards to higher expansion velocities. The emission feature starts to show up around the rest wavelength. The last spectrum from November 11 shows the  $H\alpha$  line completely in emission. The emission feature is asymmetric and has two peaks on the blue side and one peak at the red part of the feature. The rightmost peak is a bit lower than the two peaks on the left.

The spectral evolution of the prominent O I line at  $7773.0 \text{ \AA}$  is shown in Figure 5. The spectral evolution is similar to the  $H\alpha$  line as the first spectrum shows a strong absorption feature around  $-1000 \text{ km s}^{-1}$ . This absorption feature moves towards higher expansion velocities and an emission feature starts to appear. The emission feature of the last spectrum from November 11 is also asymmetric. However, the peak on the red side is the highest, in contrast to the  $H\alpha$  line. Another difference is that the absorption feature does not disappear.

To quantify the spectral evolution, we measured the velocities of the absorption feature of  $H\alpha$ ,  $H\beta$  and the O I  $7773.0 \text{ \AA}$  line as well as two Fe II lines at  $5018.4$  and  $5169.0 \text{ \AA}$  and present the results in Table 3 and Figure 6. The absorption features of all lines move towards higher expansion velocities. For the  $H\alpha$  line the last three spectra do not show a minimum in the spectrum but rather a flat part. Thus, it was not possible to determine an expansion velocity. The absorption feature of

$H\beta$  has similar expansion velocities as the  $H\alpha$  line, except for the first observation on October 31, where the  $H\alpha$  absorption feature has a higher expansion velocity than that of  $H\beta$ .

The velocities of the O I line absorption feature has slightly slower expansion velocities than the  $H\alpha$  absorption feature. The absorption feature of the O I line moves after November 5 back to smaller expansion velocities. However, we do not have a daily coverage around that time so the "maximum" could have occurred on a different day. The expansion velocities of the two Fe II lines are very similar. Nevertheless, they do not rise as high as the ones of the hydrogen lines. On November 5, the expansion velocities of the hydrogen lines are over  $1500 \text{ km s}^{-1}$ , while the ones of the lines of Fe II and O I are lower than  $1400 \text{ km s}^{-1}$ .

In addition, we measured the positions of the emission peaks of the  $H\alpha$  line in the spectrum obtained on November 11, about 13 days after the discovery to determine their velocities. We found that the bluest emission peak is located at a velocity of  $-620 \pm 10 \text{ km s}^{-1}$ . The middle peak, which is still a bit shifted to the blue, has a velocity of  $-177 \pm 14 \text{ km s}^{-1}$ . The peak at the red part of the  $H\alpha$  emission feature is located at a velocity of  $845 \pm 18 \text{ km s}^{-1}$ .

In comparison, the O I emission feature has its highest peak when the  $H\alpha$  feature has its lowest. In total, the O I  $7773.0 \text{ \AA}$  line has four peaks. The bluest peak, which is also the lowest, has a velocity of  $-576 \pm 12 \text{ km s}^{-1}$ . The velocity is similar to that of the blue peak of the  $H\alpha$  emission feature. For the second peak we determined a velocity of  $-73 \pm 20 \text{ km s}^{-1}$ . The third peak is already redshifted and presents a velocity of  $279 \pm 50 \text{ km s}^{-1}$ . The redmost peak has a velocity of about  $868 \pm 30 \text{ km s}^{-1}$ . The velocity of the red peak is practically the same as that of the respective peak of the  $H\alpha$  line. However, as already mentioned, the form of the emission feature is the opposite.

It is important to mention that the shape of the  $H\beta$  emission feature is similar to the one of the  $H\alpha$  feature. The highest peak is also located on the blue side of the feature. It has also two peaks on the blue side and one on the red side of the feature. We found that the Fe II emission features are mainly flat without any significant asymmetries or peaks.

The rightmost feature of the emission lines is the clearest and also clearly distinguishable in most of the lines. Thus, we measured the expansion velocity of the peak of these features for the lines of  $H\alpha$ ,  $H\beta$  and two O I lines at  $7773.0 \text{ \AA}$  and  $8446.3 \text{ \AA}$  and present the results in Table 4. As Figure 7 illustrates, the expansion velocity indicated by this feature decreases with time in all lines. The expansion velocity of the rightmost emission feature of the O I line at  $8664.3 \text{ \AA}$  is the highest with values larger than  $1000 \text{ km s}^{-1}$ , while the other features show very similar expansion velocities.

**TABLE 3** Expansion velocities of the absorption features of  $H\alpha$ ,  $H\beta$ , the O I line at 7773.0 Å line and two Fe II lines at 5018.4 and 5196.0 Å.

| Date   | $v_{H\alpha}$ [km s <sup>-1</sup> ] | $v_{H\beta}$ [km s <sup>-1</sup> ] | $v_{O\text{I}, 7773}$ [km s <sup>-1</sup> ] | $v_{\text{Fe II}, 5018}$ [km s <sup>-1</sup> ] | $v_{\text{Fe II}, 5169}$ [km s <sup>-1</sup> ] |
|--------|-------------------------------------|------------------------------------|---|--|--|
| Oct 31 | -1052 ± 23                          | -962 ± 37                          | -931 ± 10                                   | -986 ± 23                                      | -980 ± 23                                      |
| Nov 01 | -1255 ± 45                          | -1258 ± 62                         | -1174 ± 19                                  | -1230 ± 48                                     | -1189 ± 59                                     |
| Nov 02 | -1371 ± 17                          | -1326 ± 24                         | -1280 ± 11                                  | -1308 ± 48                                     | -1270 ± 35                                     |
| Nov 05 | -1522 ± 78                          | -1597 ± 105                        | -1390 ± 10                                  | -1320 ± 83                                     | -1334 ± 41                                     |
| Nov 07 |                                     | -1597 ± 124                        | -1317 ± 10                                  | -1404 ± 120                                    |  |
| Nov 08 |                                     | -1418 ± 124                        | -1273 ± 10                                  | -1320 ± 120                                    |  |
| Nov 11 |                                     |                                    | -1252 ± 10                                  |  |  |
| Nov 17 |                                     |                                    | -1099 ± 10                                  |  |  |

**TABLE 4** Expansion velocities of the rightmost emission features of  $H\alpha$ ,  $H\beta$  and the two O I lines at 7773.0 and 8446.3 Å.

| Date   | $v_{H\alpha}$ [km s <sup>-1</sup> ] | $v_{H\beta}$ [km s <sup>-1</sup> ] | $v_{O\text{I}, 7773}$ [km s <sup>-1</sup> ] | $v_{O\text{I}, 8446}$ [km s <sup>-1</sup> ] |
|--------|-------------------------------------|------------------------------------|---|---|
| Nov 05 | 927 ± 30                            | 956 ± 21                           | 964 ± 23                                    | 1086 ± 53                                   |
| Nov 07 | 854 ± 23                            | 882 ± 30                           | 887 ± 19                                    | 1008 ± 18                                   |
| Nov 08 | 854 ± 23                            | 857 ± 19                           | 890 ± 19                                    | 923 ± 18                                    |
| Nov 11 | 845 ± 18                            | 826 ± 24                           | 868 ± 30                                    | 870 ± 30                                    |
| Nov 17 | 831 ± 23                            |                                    | 825 ± 70                                    | 841 ± 70                                    |

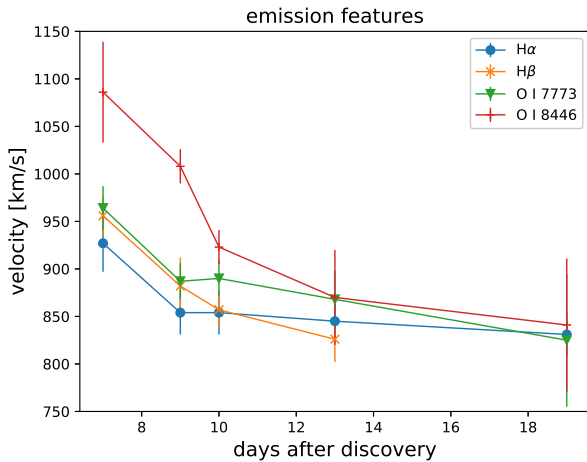


**FIGURE 7** Evolution of the expansion velocities of the rightmost emission features of four spectral lines that correspond to two different species.

### 3.3 | Interstellar absorption features

#### 3.3.1 | Atomic absorption

The intermediate resolution spectra of Nova V659 Sct show several absorption features of the interstellar medium (ISM). We added up the flux of all our eight TIGRE spectra in order

to obtain one spectrum with a higher S/N to be able to identify and measure the ISM absorption features. We found clear absorption features for the common atomic IS lines of Ca II and Na I. There is indication of both common K I lines at 7664.91 and 7698.97 Å in the spectra of Nova V659 Sct, but we cannot analyse these features since the lines are strongly blended with telluric absorption lines.

The IS absorption of Na I presented in Figure 8 shows three strong and clear subfeatures. The strongest feature in the middle seems to have another subfeature at its left side, but it is not clearly distinguishable. The vertical lines represent the rest wavelengths of the two Na I D doublet lines. One absorption feature is slightly blueshifted, while the other two features are shifted to the red.

We determined the minimum of the absorption features and measured their equivalent widths (EW). We present the results of our measurements in Table 5. The velocities of the respective features of the two Na I D lines are similar. The features of the Ca II H & K lines suffer from a very low S/N. There seems to be a substructure at the right part of the feature. However, we cannot distinguish this substructure and, therefore, determined the velocity and the equivalent width assuming just one feature. The velocity of the Ca II absorption features is comparable to the one of the middle feature of the Na I lines. There exists also interstellar absorption of K I. However, these features are



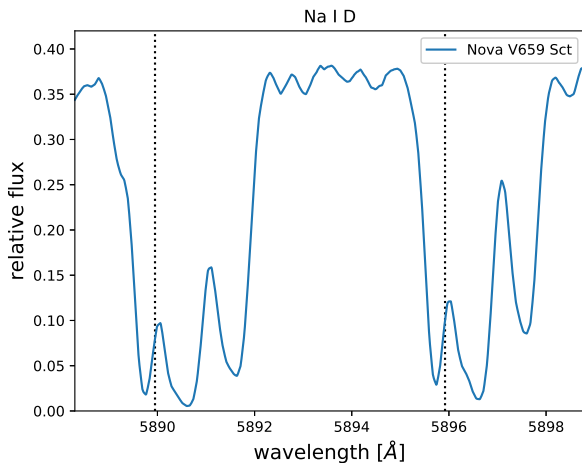


**FIGURE 8** Interstellar absorption features of Na I in Nova V659 Sct. Three clear subfeatures are visible.

**TABLE 5** Velocities and equivalent widths (EW) of the atomic interstellar absorption features of Ca II and Na I found in Nova V659 Sct.

| Ion   | wavelength [Å] | velocity [km s <sup>-1</sup> ] | EW [mÅ]    |
|-------|----------------|--------------------------------|------------|
| Ca II | 3933.66        | 21.4 ± 2.3                     | 1649 ± 100 |
| Ca II | 3968.47        | 22.1 ± 2.5                     | 1014 ± 55  |
| Na I  | 5889.95        | -9.5 ± 0.6                     | 641 ± 40   |
|       |                | 30.3 ± 0.4                     | 1315 ± 100 |
|       |                | 84.1 ± 0.5                     | 599 ± 60   |
| Na I  | 5895.92        | -10.1 ± 0.6                    | 493 ± 20   |
|       |                | 30.0 ± 0.6                     | 1098 ± 100 |
|       |                | 86.8 ± 0.6                     | 440 ± 30   |

strongly blended with telluric lines, and it is impossible to perform any measurements.

### 3.3.2 | Diffuse interstellar bands

The intermediate resolution spectra of Nova V659 Sct contain several features of diffuse interstellar bands (DIB). We measured the equivalent widths of the features by integrating over the features. In addition, we determined the position of the minima in order to estimate the velocity of the respective DIB features. We used for that the rest wavelengths for the DIBs given in Hobbs et al. (2009). Inspecting the spectra of Nova V659 Sct, we could identify several DIBs. The measured velocities and equivalent widths (EW) of the features are given in Table 6. DIB 5780 is the strongest DIB with the highest EW that we found. All of the DIBs found in the spectra of Nova V659 Sct were also present in the spectra

**TABLE 6** Identified DIBs in the spectra of Nova V659 Sct and their respective velocities and equivalent widths (EW).

| Feature  | velocity [km s <sup>-1</sup> ] | EW [mÅ]  |
|----------|--------------------------------|----------|
| DIB 5780 | 19.2 ± 7.8                     | 602 ± 23 |
| DIB 5797 | -6.7 ± 5.2                     | 238 ± 7  |
| DIB 5850 | -1.0 ± 4.6                     | 69 ± 2   |
| DIB 6196 | 2.1 ± 4.8                      | 52 ± 2   |
| DIB 6203 | 31.6 ± 7.3                     | 276 ± 4  |
| DIB 6379 | -14.7 ± 1.5                    | 69 ± 1   |
| DIB 6614 | 8.6 ± 4.1                      | 238 ± 8  |
| DIB 6660 | -16.3 ± 2.9                    | 22 ± 1   |
| DIB 7562 | -5.1 ± 6.4                     | 171 ± 3  |
| DIB 7581 | -11.1 ± 7.1                    | 36 ± 2   |

the other two novae that we observed with the TIGRE telescope (Jack & Schröder, 2019). There are two DIBs (5850 and 7581) that are "new" in Nova V659 Sct. In general, the EWs of the DIBs are significantly higher in the spectra of Nova V659 Sct, which agrees with the high galactic reddening of  $E(B-V) = 0.9$  found by Sokolovsky et al. (2019). The values for the velocities are somewhat distributed over a larger range from -14.7 to 31.6 km s<sup>-1</sup>. However, the S/N of the spectra was not very high, and it was difficult to determine the position of the minimum and, thus, the velocity of the DIB features.

## 4 | SUMMARY AND CONCLUSIONS

We obtained a series of eight optical spectra (3,800 to 8,800 Å) of the Nova V659 Sct during the different phases of its outburst with our robotic 1.2 m TIGRE telescope and its intermediate resolution ( $R \approx 20,000$ ) HEROS spectrograph. Using the MMRD relation we could place the Nova at a distance of about 7.5 kpc. A thorough line identification was performed finding lines of H I, Fe II, O I, Na I and Ca II, among others. The absorption features of the H $\alpha$  and the O I 7773.0 Å lines move during the first days of the spectral evolution to higher expansion velocities. The emission features are asymmetric with three peaks for the H $\alpha$  line or four peaks for the O I line. While in the H $\alpha$  line the rightmost peak was the lowest, it was the strongest in the O I line. The position of the outermost peaks are about the same. The expansion velocity of the rightmost emission feature is decreasing in time.

This Nova went from optically thick absorption line spectrum into optically thin nebular phase very quickly, indicating a small envelope mass. This is supposed to be typical for a more evolved system with a relatively large WD mass, as such erupting more frequently with only small amounts of accreted hydrogen igniting easily. In comparison with the Novae V339

Del and V5668 Sgr, the absorption features of the spectral lines in V659 Sct show higher expansion velocities.

Thanks to the resolution of the spectra of Nova V659 Sct, we were able to study the absorption features of the interstellar medium. Concerning the atomic ISM absorption features, we found that both sodium D lines show a substructure with three main components. Interstellar absorption of Ca II is present, but it is not possible to distinguish any substructures due to the low S/N in that part of the spectra. We also identified the features of both K I lines, but they are strongly blended with telluric absorption lines. Several DIBs were identified in the spectra of Nova V659 Sct, even two more than in Novae V339 Del and V5668 Sgr. We determined the velocities and the equivalent widths of all DIB features. The DIBs are relatively strong due to high galactic reddening (e.g. absorption), and this is confirmed by the high value of  $E(B - V) = 0.9$  mentioned earlier.

## ACKNOWLEDGMENTS

The authors are grateful for financial support by the joint bilateral project CONAcYT-DFG No. 278156.

We acknowledge with thanks the variable star observations from the AAVSO International Database contributed by observers worldwide and used in this research.

## REFERENCES

- Bode, M. F. 2010, February, *AN*, 331, 160. doi:  
 Bode, M. F., & Evans, A. 2008, *Classical Novae*. Cambridge University Press.  
 De Gennaro Aquino, I., Schröder, K.-P., Mittag, M. et al. 2015, September, *A&A*, 581, A134. doi:  
 della Valle, M., & Livio, M. 1995, October, *ApJ*, 452, 704. doi:  
 Gallagher, J. S., & Starrfield, S. 1978, *ARA&A*, 16, 171-214. doi:  
 Green, G. M., Schlafly, E., Zucker, C., Speagle, J. S., & Finkbeiner, D. 2019, December, *ApJ*, 887(1), 93. doi:  
 Hobbs, L. M., York, D. G., Thorburn, J. A. et al. 2009, November, *ApJ*, 705(1), 32-45. doi:  
 Jack, D., Mittag, M., Schröder, K.-P. et al. 2015, August, *MNRAS*, 451, 4104-4113. doi:  
 Jack, D., Robles Pérez, J. d. J., De Gennaro Aquino, I. et al. 2017, January, *Astronomische Nachrichten*, 338(1), 91-102. doi:  
 Jack, D., & Schröder, K. P. 2019, October, *Rev. Mexicana Astron. Astrofis.*, 55, 141-149. doi:  
 Kochanek, C. S., Shappee, B. J., Stanek, K. Z. et al. 2017, October, *PASP*, 129(980), 104502. doi:  
 Nishiyama, K., Kabashima, F., & Nishimura, H. 2019, October, *Central Bureau Electronic Telegrams*, 4690, 1.  
 Pavana, M., Anupama, G. C., & Kumar, S. P. 2019, October, *The Astronomer's Telegram*, 13245, 1.  
 Payne-Gaposchkin, C. 1964, *The Galactic Novae*. Dover Publications.  
 Schmitt, J. H. M. M., Schröder, K.-P., Rauw, G. et al. 2014, October, *AN*, 335, 787. doi:

- Shappee, B. J., Prieto, J. L., Grupe, D. et al. 2014, June, *ApJ*, 788(1), 48. doi:  
 Sokolovsky, K. V., Aydi, E., Chomiuk, L. et al. 2019, October, *The Astronomer's Telegram*, 13252, 1.  
 Stanek, K. Z., & Kochanek, C. S. 2019, October, *Transient Name Server Discovery Report*, 2019-2216, 1.  
 Starrfield, S., Iliadis, C., & Hix, W. R. 2016, May, *PASP*, 128(963), 051001. doi:  
 Williams, S. C., Darnley, M. J., Healy, M. W., Murphy-Glasyher, F. J., & Ransome, C. L. 2019, October, *The Astronomer's Telegram*, 13241, 1.



## APPENDIX A: OBSERVATION DETAILS

We present the details of our TIGRE observations in Table A1 . The start of the observations is given in UT. The exposure times were either 30 minutes or one hour. The mean S/N is taken from the spectrum of the red channel.

**TABLE A1** Details of the TIGRE observations.

| <b>Date<br/>(UT)</b> | <b>Time<br/>(UT)</b> | <b>Julian Date</b> | <b>Airmass</b> | <b>Avg. Seeing<br/>[arcsec]</b> | <b>Exposure<br/>[sec]</b> | <b>Mean S/N</b> |
|----------------------|----------------------|--------------------|----------------|---------------------------------|---------------------------|-----------------|
| <b>Oct 31</b>        | 00 : 52 : 24         | 2458787.536389     | 1.375994       | 1.440504                        | 1800                      | 90.2            |
| <b>Nov 01</b>        | 00 : 51 : 44         | 2458788.535929     | 1.389399       | 3.494088                        | 3600                      | 42.7            |
| <b>Nov 02</b>        | 00 : 50 : 56         | 2458789.535371     | 1.402655       | 1.983384                        | 1800                      | 63.0            |
| <b>Nov 05</b>        | 01 : 21 : 39         | 2458792.556700     | 1.63851        | 1.524744                        | 3600                      | 55.3            |
| <b>Nov 07</b>        | 00 : 48 : 45         | 2458794.533852     | 1.48339        | 2.543112                        | 3600                      | 47.0            |
| <b>Nov 08</b>        | 00 : 48 : 48         | 2458795.533888     | 1.505066       | 1.689012                        | 3600                      | 60.1            |
| <b>Nov 11</b>        | 00 : 47 : 06         | 2458798.532709     | 1.564179       | 1.302912                        | 3600                      | 47.3            |
| <b>Nov 17</b>        | 00 : 59 : 45         | 2458804.541489     | 1.858462       | 1.798992                        | 1800                      | 9.6             |